Van der Waals Complexes between Unsaturated Hydrocarbons and Boron Trifluoride: An Infrared and *ab Initio* Study of Ethene·BF_3 and Propene·BF_3

W. A. Herrebout and B. J. van der Veken*

Contribution from the Department of Chemistry, Universitair Centrum Antwerpen, Groenenborgerlaan 171, B-2020 Antwerpen, Belgium

Received June 9, 1997[⊗]

Abstract: The mid-infrared (4000−400 cm^{-1}) spectra of ethene/BF_3 and propene/BF_3 mixtures, dissolved in liquid argon (93−125K) and in liquid nitrogen (80−118K) are discussed. In all spectra, the formation of a 1:1 van der Waals complex, in which the electron deficient BF_3 molecule binds to the C═C double bond, was observed. Using spectra recorded at different temperatures, the complexation enthalpy ΔH^o for ethene·BF_3 was determined to be -10.0 ± 0.2 kJ mol^{-1} in liquid argon and -5.4 ± 0.3 kJ mol^{-1} in liquid nitrogen, while for propene·BF_3 the ΔH^o are -11.8 ± 0.2 and -6.9 ± 0.3 kJ mol^{-1}, respectively. For both complexes a converged structure and the harmonic vibrational frequencies were calculated using *ab initio* calculations at the MP2/6-31+G* level.

Introduction

Typically for an electron deficient molecule, boron trifluoride exhibits unusually strong interactions with other molecules. As a result, BF_3 readily forms stable adducts with electron donors, particularly with nitrogen and oxygen bases.[1−3] These adducts have been studied using a variety of techniques.[4−6] Under cryogenic conditions also a number of weakly bound complexes have been studied to date. For instance, molecular beam high-resolution infrared spectra of the adduct of BF_3 with Ne, Ar, Kr, N_2, and CO have been observed by Takami and co-workers,[7−11] and similar complexes involving HCN and HC-CCN were described by Kerstel et al.[12] Also, the molecular beam microwave spectra of BF_3 complexes with a variety of Lewis bases have been reported,[13−18] and the complexes with N_2, CO, and H_2O, as well as the BF_3 dimer, have been identified in matrix isolation infrared studies.[19−22]

For some time, we have been using cryosolutions in the study of van der Waals complexes of BF_3.[23,24] For the Lewis bases studied up to now, the complexation occurs via a free electron pair of the base molecule. It is clear that similar interactions may be expected with electron donor molecules that contain unsaturated bonds. To our knowledge, no information on species of this kind has yet been obtained. Therefore, we have investigated the formation of complexes of ethene and propene with BF_3 in cryosolutions, using infrared spectroscopy. In the paragraphs below, we will describe the spectra observed and derive the stoichiometry of the complexes and their complexation enthalpy. Structural models for the complexes have been obtained by *ab initio* calculations, and the results will be used to interpret the observations.

Experimental Section

The samples of ethene (99.5+%), propene (99+%), and boron trifluoride (CP grade) were purchased from Aldrich and Union Carbide, respectively. The solvent gases, argon and nitrogen, were supplied by L'Air Liquide and have a stated purity of 99.9999%. In the spectra of ethene, propene, argon, and nitrogen, no impurities could be detected, while small amounts of SiF_4 were present as an impurity in the BF_3 used. All gases were used without further purification.

The infrared spectra were recorded on a Bruker IFS 66v or a Bruker 113v Fourier Transform spectrometer, using a Globar source in combination with a Ge/KBr beamsplitter and a broadband MCT detector. The interferograms were averaged over 200 scans, Happ Genzel apodized, and Fourier transformed using a zero filling factor of 4, to yield spectra at a resolution of 0.5 cm^{-1}. A detailed description of the liquid noble gas setup has been given before.[25]

⊗ Abstract published in *Advance ACS Abstracts,* October 1, 1997.

(1) Greenwood, N. N.; Martin, R. L. *Q. Rev.* **1954**, *8*, 1−39.
(2) Olah, G. *Friedel-Crafts and Related Reactions*; Interscience: New York, 1963.
(3) Greenwood, N. N.; Earnshaw, A. *Chemistry of the Elements*, Pergamon Press: Oxford, 1984; p 220.
(4) Nxumalo, L. M.; Ford, T. A. *S. Afr. J. Chem.* **1995**, *48*, 30−38 and references therein.
(5) Nxumalo, L. M.; Ford, T. A. *J. Mol. Struct.* **1996**, *369*, 115−126 and references therein.
(6) Nxumalo, L. M.; Andrzejak, M.; Ford, T. A. *J. Chem. Inf. Comput. Sci.* **1996**, *36*, 377−384 and references therein.
(7) Takami, M.; Ohshima, Y.; Yamamoto, S.; Matsumoto, Y. *Faraday Discuss. Chem. Soc.* **1988**, *86*, 1−12.
(8) Matsumoto, Y.; Ohshima, Y.; Takami, M. *J. Chem. Phys.* **1989**, *90*, 7017−7021.
(9) Lee, G.; Matsuo, Y.; Takami, M.; Matsumoto, Y. *J. Chem. Phys.* **1992**, *96*, 4079−4087.
(10) Lee, G.; Takami, M. *J. Chem. Phys.* **1993**, *98*, 3612−3619.
(11) Lee, G.; Takami, M. *J. Mol. Struct.* **1995**, *352/353*, 417−422.
(12) Kerstel, E. R. Th.; Pate, B. H.; Mentel, T. F.; Yang, X.; Scoles, G. *J. Chem. Phys.* **1994**, *101*, 2762−2771.
(13) Janda, K. C.; Bernstein, L. S.; Steed, J. M.; Novick, S. E.; Klemperer, W. *J. Am. Chem. Soc.* **1978**, *100*, 8074−8079.
(14) Leopold, K. R.; Fraser, G. T.; Klemperer, W. *J. Am. Chem. Soc.* **1984**, *106*, 897−899.
(15) Cassoux, P.; Kuczkowski, R. L.; Serafini, A. *Inorg. Chem.* **1977**, *16*, 3005−3008.
(16) Lobue, J. M.; Rice, J. K.; Blake, T. K.; Novick, S. E. *J. Chem. Phys.* **1986**, *85*, 4261−4268.
(17) Legon, A. C.; and Warner, H. E. *J. Chem. Soc., Chem. Commun.* **1991**, *19*, 1397−1399.
(18) Campbell, E. J.; Phillips, J. A.; Goodfriend, H.; Grushow, A.; Canagaratna, M.; Almlöf, J.; Leopold, K. R. The 49th Ohio State University International Symposium on Molecular Spectroscopy, 1994.
(19) Gebicki, J.; Liang, J. *J. Mol. Struct.* **1984**, *117*, 283−286.
(20) Evans, D. G.; Yeo, G. A.; Ford, T. A. *Faraday Discuss. Chem. Soc.* **1988**, *86*, 55−63.
(21) O'Neill, F. M. M.; Yeo, G. A.; Ford, T. A. *J. Mol. Struct.* **1988**, *173*, 337−348.
(22) Truscott, C. S.; Ault, B. S. *J. Mol. Struct.* **1987**, *157*, 67−71.
(23) Sluyts, E. J.; Van der Veken, B. J. *J. Am. Chem. Soc.* **1996**, *118*, 440−445.
(24) Sluyts, E. J.; Van der Veken, B. J., *unpublished results*.
(25) Van der Veken, B. J. Infrared Spectroscopy in liquefied noble gases. In *Low Temperature Molecular Spectroscopy*; Fausto, R., Ed.; Kluwer Academic Publishers: Dordrecht, 1996.

S0002-7863(97)01887-8 CCC: $14.00

Computational Details

Ab initio calculations were performed using the Gaussian 94 package.[26] For all calculations, the correlation energy was calculated using second-order Møller−Plesset perturbation theory, including explicitely all electrons, while the Berny optimization[27,28] was used with the tight convergence criteria. For all calculations the 6-31+G* basis set was used.

The complexation energies of the weak complexes were calculated by subtracting the calculated energies of the monomers from that of the complex, and these energies were corrected for basis set superposition error (BSSE) using the counterpoise correction method described by Boys and Bernardi.[29] For the equilibrium geometries, the vibrational frequencies and the corresponding infrared intensities were calculated using standard harmonic force fields.

Results and Discussion

1. Vibrational Spectra. For BF_3 and C_2H_4 we will use the standard numbering scheme to identify the vibrational modes. Especially for C_2H_4 in this way the use of oversimplified descriptions is avoided. For propene the numbering scheme is less instructive, and for this species we have, where judged necessary, supplemented the numbering scheme with a description in terms of internal coordinates. Because the complexes are very weak, their vibrations can easily be classified either as modes localized in the monomers or as van der Waals modes. The former will be described using the corresponding monomer symbols.

A. Monomer Spectra. The vibrational spectra of boron trifluoride and ethene in cryosolutions have been described in detail elsewhere[23,30−31] and will not be discussed here. To our knowledge, no infrared data of propene in cryosolution has yet been reported. Therefore, the frequencies of propene in liquid argon solution (LAr) and their assignments, obtained by comparison with earlier studies,[32] are summarized in Table 1.

As propene has been used in its natural isotopic abundance, weak bands due to the $^{13}CH_3CH{=}CH_2$, the $CH_3{}^{13}CH{=}CH_2$, and the $CH_3CH{=}{}^{13}CH_2$ isotopomers must be expected. For example, on the low-frequency side of the C=C stretch at 1651 cm^{-1}, weak bands due to the $CH_3{}^{13}CH{=}CH_2$ and $CH_3CH{=}{}^{13}CH_2$, isotopomers appear at 1628 and 1622 cm^{-1}, respectively. For $^{13}CH_3CH{=}CH_2$, a band with comparable intensity must be expected. However, no separate band due to this species was observed, presumably because it is strongly overlapped by the band of the mother isotope.

B. Ethene/BF_3. Upon complexation, the antisymmetric stretch, $\nu_3{}^{BF_3}$, and the out of plane deformation, $\nu_2{}^{BF_3}$, of boron trifluoride show a considerable red shift.[4−6,19−23] Thus, the formation of a complex can be confirmed by the occurence of new bands in the 1500−1400 and 700−600 cm^{-1} regions. For ethene/BF_3 mixtures in LAr, such bands were indeed observed. In Figure 1A, the $\nu_3{}^{BF_3}$ region of BF_3 of a solution containing

Table 1. Observed[a] Frequencies (cm^{-1}) and Assignments for Propene

liq argon	rel int	gas	ν_i	approximate description
3107	w			$\nu_6 + \nu_7$
3089	vs	3091.4	ν_1	$=CH_2$ asym stretch
3074	s			$\nu_6 + \nu_{16}$
3025	m, sh			$\nu_6 + \nu_9$
3020	s		ν_2	=CH stretch
3004	m			
2987	vs	2991.0	ν_3	$=CH_2$ sym stretch
2971	s		ν_4	CH_3 asym stretch
2949	vs	2954.1	ν_{15}	$CH_2=$ asym stretch
2926	vs	2931.8	ν_5	CH_3 sym stretch
2909	vw			$2\nu_7$
2894	s			$\nu_7 + \nu_{16}$
2860	s	2867.8		$2\nu_{16}$
2853	m, sh			$\nu_8 + \nu_{16}$
2825	w			$\nu_7 + \nu_9$
2817	vw			$\nu_9 + \nu_{16}$
2809	vw			
2786	m			$\nu_{13} + \nu_{14} + \nu_{16}$
2730	m	2737.0		$2\nu_{13} + \nu_{19}$
2709	w			
2622	w			
2580	vw			$2\nu_{10}$
2562	w			$\nu_6 + \nu_{19}$
2542	w			
2476	w			
2466	w			
2387	w			$\nu_7 + \nu_{12}$
2375	vw			$\nu_7 + \nu_{13}$
2349	vw			$\nu_8 + \nu_{12}$
2331	vw			$\nu_8 + \nu_{13}$
2290	w			$\nu_{10} + \nu_{18}$
2229	w			$\nu_{10} + \nu_{12}$
2214	vw			$\nu_{10} + \nu_{13}$
2084	vw			$\nu_6 + \nu_{14}$
2077	vw			
2031	m	2033.2		$\nu_{17} + \nu_{18}$
1976	w			$2\nu_{18}$
1954	vw			$\nu_{17} + \nu_{19}$
1925	vw			$\nu_{12} + \nu_{18}$
1896	vw			$\nu_{18} + \nu_{19}$
1885	vw			$\nu_7 + \nu_{14}$
1869	vw			$\nu_{14} + \nu_{16}$
1852	w			$\nu_{12} + \nu_{13}$
1845	w			$2\nu_{12}$
1824	s	1828.5		$2\nu_{13}$
1651	vs	1653.0	ν_6	C=C stretch
1268	w		ν_6*	C=C stretch $^{13}CH_2{=}CHCH_3$
1622	w		ν_6*	C=C stretch $CH_2{=}{}^{13}CHCH_3$
1598	vw			
1568	m	1567.4		$\nu_{18} + \nu_{20}$
1499	vw			$\nu_{13} + \nu_{20}$
1488	w			$\nu_{19} + \nu_{20}$
1474	w, sh			$\nu_{14} + \nu_{17}$
1455	vs	1457.7	ν_7	CH_3 asym deformation
1439	s	1442.4	ν_{16}	CH_3 asym deformation
1416	m		ν_8	$=CH_2$ deformation
1375	m	1378.1	ν_9	CH_3 sym deformation
1365	vw, sh			$\nu_{14} + \nu_{12}$
1345	vw			$\nu_{14} + \nu_{13}$
1297	vw	1297.8	ν_{10}	C=CH in-plane deformation
1240	w			$\nu_{17} + \nu_{21}$
1171	w		ν_{11}	$=CH_2$ rocking
1153	vw			$2\nu_{20}$
1043	m	1044.8	ν_{17}	CH_3 rocking
990	vs	991.4	ν_{18}	C=CH out-of-plane
935	vs		ν_{12}	CH_3 rocking
918	s, sh		ν_{13}	C−C stretch
910	vs	912.4	ν_{19}	$=CH_2$ wagging
577	vs	576.3	ν_{20}	$=CH_2$ twist
430	m		ν_{14}	C=C−C deformation
177	w		ν_{21}	CH_3 torsion

[a] Abbreviations: vs, very strong; s, strong; m, medium; w, weak; vw, very weak; sh, shoulder.

(26) Gaussian 94, Revision B.2, M. J. Frisch, G. W. Trucks, H. B. Schlegel, P. M. W. Gill, B. G. Johnson, M. A. Robb, J. R. Cheeseman, T. Keith, G. A. Petersson, J. A. Montgomery, K. Raghavachari, M. A. Al-Laham, V. G. Zakrzewski, J. V. Ortiz, J. B. Foresman, J. Cioslowski, B. B. Stefanov, A. Nanayakkara, M. Challacombe, C. Y. Peng, P. Y. Ayala, W. Chen, M. W. Wong, J. L. Andres, E. S. Replogle, R. Gomperts, R. L. Martin, D. J. Fox, J. S. Binkley, D. J. Defrees, J. Baker, J. P. Stewart, M. Head-Gordon, C. Gonzalez, and J. A. Pople, Gaussian, Inc., Pittsburgh, PA, 1995.

(27) Schlegel, H. B. In *Ab Initio Methods in Quantum Chemistry*; Lawley, K. P., Ed.; Wiley: Chichester, 1987; Part 1, p 249.

(28) Peng, C.; Ayala, P. Y.; Schlegel, H. B.; Frish, M. J. *J. Comput. Chem.* **1996**, 17, 49−56.

(29) Boys, S. B.; Bernardi, F. *Mol. Phys.* **1970**, *19*, 553−566.

(30) Brock, A.; Mina-Camilde, N.; Manzanares I. C. *J. Phys. Chem.* **1994**, *98*, 4800−4808.

(31) Herrebout, W. A.; Everaert, G. P.; Van der Veken, B. J.; Bulanin, M. O. *J. Chem. Phys.*, accepted for publication.

(32) Sverdlov, L. M.; Kovner, M. A.; Krainov, E. P. *Vibrational Spectra of Polyatomic Molecules*; Wiley: New York, 1974, and references therein.

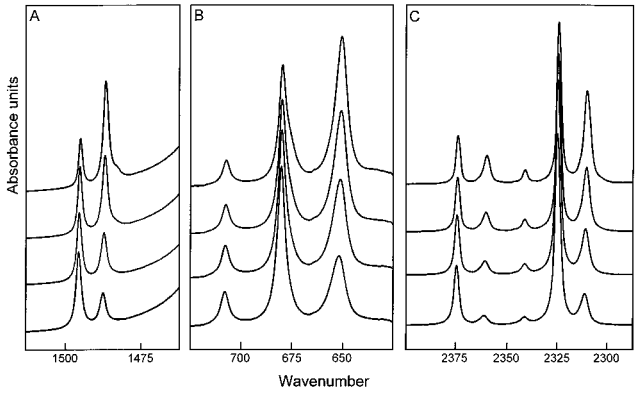

Figure 1. Details of the mid-infrared spectra of ethene/BF_3 mixtures dissolved in liquefied argon: (A) the $\nu_3^{^{10}BF_3}$ region; (B) the $\nu_2^{BF_3}$ region; (C) the $\nu_1^{BF_3} + \nu_3^{BF_3}$ region. From top to bottom, the temperature of the solutions increases, from 84.1 to 98.2 K, from 93.1 to 100.7 K and from 91.9 to 105.2 K, respectively.

Table 2. Observed Vibrational Frequencies (cm^{-1}) and Complexation Shifts (cm^{-1}) for C_2H_4, $^{10}BF_3$, $^{11}BF_3$, $C_2H_4{\cdot}^{10}BF_3$, and $C_2H_4{\cdot}^{11}BF_3$ Dissolved in Liquid Argon

BF$_3$ Submolecule

assignment	$^{11}BF_3$	$C_2H_4{\cdot}^{11}BF_3$		$^{10}BF_3$	$C_2H_4{\cdot}^{10}BF_3$	
$\nu_1^{BF_3} + \nu_3^{BF_3} + \nu_4^{BF_3}$	2798	2782	−16	2851		
$\nu_1^{BF_3} + \nu_3^{BF_3}$	2325	2310	−15	2375	2360	−15
$\nu_3^{BF_3}$	1445	1438	−7	1494	1487	−7
$\nu_1^{BF_3} + \nu_4^{BF_3}$	1358	1351	−7	1358	1351	−7
$\nu_1^{BF_3}$	−[a]	878	−3	−[a]	878	−3
$\nu_2^{BF_3}$	681	651	−30	709	679[b]	−30
$\nu_4^{BF_3}$	474	−	−	474	−	−

Ethene Submolecule

assignment	C_2H_4	$C_2H_4{\cdot}BF_3$	
$\nu_3 + \nu_{12}$	−	2774	
ν_2	−[c]	1621	
$\nu_7 + \nu_8$	1886	1909	+23

[a] Not infrared active, Raman gas phase frequency at 888 cm^{-1}. [b] Due to the overlap with the 681 cm^{-1} band, no accurate frequency can be obtained for the $\nu_2^{BF_3}$ fundamental in $C_2H_4{\cdot}^{10}BF_3$. [c] Not infrared active, Raman gas phase frequency at 1625 cm^{-1}.

approximately 1.0×10^{-4} M BF_3 and 5.0×10^{-3} M C_2H_4 is shown at several temperatures between 84 and 98 K. The band at 1494 cm^{-1} is the $^{10}BF_3$ monomer absorption while the band at 1487 cm^{-1} is caused by a complex. The presence of the very intense ν_{12} of ethene at 1439 cm^{-1} prevented the observation of the corresponding bands due to the ^{11}B isotopomer.

In Figure 1B, the $\nu_2^{BF_3}$ region of a solution containing approximately 0.4×10^{-3} M BF_3 and 5.0×10^{-3} M C_2H_4 is shown. The bands at 709 and 681 cm^{-1} are due to monomer $^{10}BF_3$ and $^{11}BF_3$. The band at 651 cm^{-1} and the shoulder near 679 cm^{-1} are assigned to the adduct with $^{11}BF_3$ and $^{10}BF_3$, respectively.

Complex bands have also been observed for combination bands involving $\nu_2^{BF_3}$ or $\nu_3^{BF_3}$. This is illustrated in Figure 1C, where the $\nu_1^{BF_3} + \nu_3^{BF_3}$ region of the spectra is shown. New bands due to a complex can be seen to occur at 2360 and 2310 cm^{-1}. Also for the $\nu_1^{BF_3} + \nu_4^{BF_3}$ and the $\nu_1^{BF_3} + \nu_3^{BF_3} + \nu_4^{BF_3}$ combinations, complex bands were observed. The frequencies of these bands and the complexation shifts defined as $\nu_{complex} - \nu_{monomer}$ are collected in Table 2.

For ethene, only a limited number of fundamentals is infrared active. Of these, in the C−H stretching region no bands signaling the formation a complex were observed. For the concentrations of ethene used in this study, the region of $\nu_7^{C_2H_4}$ is completely saturated, so that for this mode no complex band could be observed. However, near the band at 1886 cm^{-1}, assigned to $\nu_7^{C_2H_4} + \nu_8^{C_2H_4}$ in monomer ethene, a weak complex band was observed at 1909 cm^{-1}.

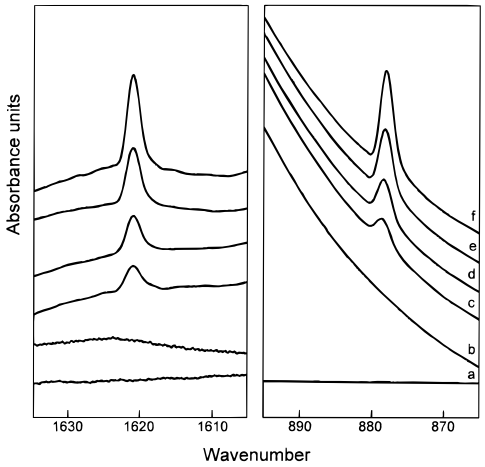

Figure 2. The $\nu_{C=C}$ (A) and the $\nu_5^{BF_3}$ (B) region for a solution containing ethene (a), BF_3 (b) and a typical ethene/BF_3 mixture (c−f). From *c* to *f*, the temperature of the mixed solution decreases from 105.2 to 91.9 K.

In the spectra of BF_3/CO mixtures in LAr[23] a weak band at 879 cm^{-1} was assigned to $\nu_1^{BF_3}$ in $BF_3{\cdot}CO$. This mode is forbidden in monomer BF_3, but has induced intensity in the complex. An analogous phenomenon was observed for $\nu_2^{C_2H_4}$ and $\nu_3^{C_2H_4}$ of ethene·HCl in LAr and in liquid nitrogen, LN_2.[31] The appearance of induced bands was studied here using solutions containing relatively large concentrations of both C_2H_4 and BF_3. In Figure 2, the 1630−1610 and the 890−870 cm^{-1} regions of the spectra, recorded at temperatures between 92 and 105.2 K, are compared. In both regions, a weak band can be observed, at 1621 and at 878 cm^{-1}, respectively. The former is the $\nu_2^{C_2H_4}$ of the ethene moiety, the latter is the $\nu_1^{BF_3}$ mode. As before, the presence of these bands proves the formation of a complex and indicates that the symmetry of the complex is lower than that of the monomers.

In the spectra shown in Figure 1A, a weak feature can be observed near 1484 cm^{-1}. In analogy with $BF_3{\cdot}CO$,[23] we assign this band to a higher complex, involving one BF_3 and two ethene molecules. Even when a large excess of ethene was used, however, no bands due to such species were observed in the $\nu_2^{BF_3}$ region. The formation of a 1:2 complex, therefore, is not confirmed by other observations.

To complete the analysis, the infrared spectra of ethene/BF_3 mixtures dissolved in liquid nitrogen were investigated. Also for these solutions, the appearance of new bands indicated the formation of a complex. Because of the similarity with the argon solutions, no detailed description of these bands will be given. However, it was observed that for similar concentrations of ethene and BF_3, the intensities of the complex observed bands in LN_2 solutions are much smaller than those observed for the solutions in LAr. This suggests that in LN_2 the complex is less stable than in LAr. This will be confirmed below.

C. Propene/BF_3. Inspection of the spectra of propene/BF_3 mixtures in LAr revealed a large number of new bands that must be assigned to a complex between propene and BF_3. The observed frequencies, their assignments, and the complexation shifts are summarized in Table 3. In view of the large number of splittings observed, only the more important of them will be discussed in detail.

In Figure 3, the 1500−1400 and the 2400−2275 cm^{-1} regions of mixed solutions and that of a solution containing only propene or BF_3 are compared. In the region of $\nu_3^{BF_3}$ for the mixed solutions, weak complex bands are observed at 1484 and 1433

Table 3. Observed Vibrational Frequencies (cm^{-1}) and Complexation Shifts (cm^{-1}) for Propene·$^{10}BF_3$ and Propene·$^{11}BF_3$ Dissolved in Liquid Argon

BF_3 Submolecule

assignment	$^{11}BF_3$	propene·$^{11}BF_3$		$^{10}BF_3$	propene·$^{10}BF_3$	
$\nu_1^{BF_3} + \nu_3^{BF_3} + \nu_4^{BF_3}$	2797	2776	−21			
$\nu_1^{BF_3} + \nu_3^{BF_3}$	2326	2308	−18	2376	2357	−18
$\nu_3^{BF_3} + \nu_4^{BF_3}$	1921	1908	−13	1974	1960	−14
$\nu_3^{BF_3}$	1444	1433	−11	1494	1483	−11
$\nu_1^{BF_3} + \nu_4^{BF_3}$	1358	1348	−10	1358	1348	−10
$\nu_1^{BF_3}$	−[a]	876	−8	−[a]	876	−8
$\nu_2^{BF_3}$	680	640	−40	707	664	−43
$\nu_4^{BF_3}$	474	472	−2	474	472	−2

Propene Submolecule

assignment	propene	propene·BF_3	
$\nu_6 + \nu_{19}$	2562	2572	+10
$\nu_9 + \nu_{13}$	2230	2233	+3
$\nu_{10} + \nu_{13}$	2214	2217	+3
$\nu_{17} + \nu_{18}$	2031	2043	+12
$2\nu_{18}$	1975	1995	+20
$\nu_{12} + \nu_{18}$	1925	1936	+11
$\nu_{13} + \nu_{19}$	1896	1916	+20
$\nu_{12} + \nu_{13}$	1852	1856	+4
$2\nu_{12}$	1846	1850	+4
$2\nu_{13}$	1824	1832	+8
ν_6	1651	1647	−4
ν_6* $CH_3CH{=}{}^{13}CH_2$	1628	1624	−4
ν_6** $CH_3{}^{13}CH{=}CH_2$	1622	1618	−4
ν_9	1375	1376	+1
ν_{17}	1043	1047	+4
ν_{18}	990	1000	+10
ν_{12}	934	936	+2
ν_{13}	918	921	+3
ν_{19}	910	925	+15
ν_{20}	576	591	+15

[a] Not infrared active, Raman gas phase frequency at 888 cm^{-1}.

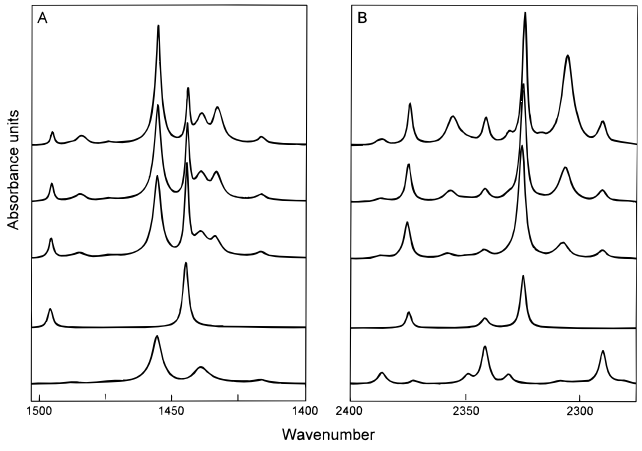

Figure 3. Details of the mid-infrared spectra of propene/BF_3 mixtures dissolved in liquefied argon : (A) the $\nu_3^{^{10}BF_3}$ region; (B) the $\nu_1^{BF_3} + \nu_3^{BF_3}$ region. The lower two spectra were recorded from solutions containing only BF_3 and propene, respectively. For the other spectra, the temperature of the solutions increases from top to bottom, from 95.9 to 116.9 K (A), and from 86.4 to 95.3 K (B), respectively.

cm^{-1}. The $\nu_1^{BF_3} + \nu_3^{BF_3}$ combination gives rise to bands in the 2400−2275 cm^{-1} region, and complex bands occur approximately 18 cm^{-1} red shifted from the monomer bands, as can be seen in Figure 3B.

On the low-frequency side of the $\nu_2^{BF_3}$ isotopic doublet, complex bands appear at 664 and 640 cm^{-1}. Comparison with ethene·BF_3 shows that the complexation shifts of these modes in the propene complex are somewhat larger, suggesting that the propene complex is more stable. This will be confirmed below.

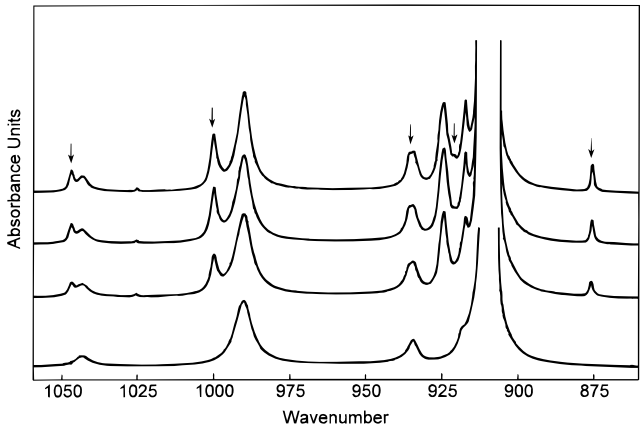

Figure 4. The 1050−875 cm^{-1} region of a propene/BF_3 mixture dissolved in liquefied argon. The bottom spectrum was recorded from a solution containing only propene. For the other spectra the temperature of the solution increases from top to bottom : 91.0, 96.3 and 100.6 K.

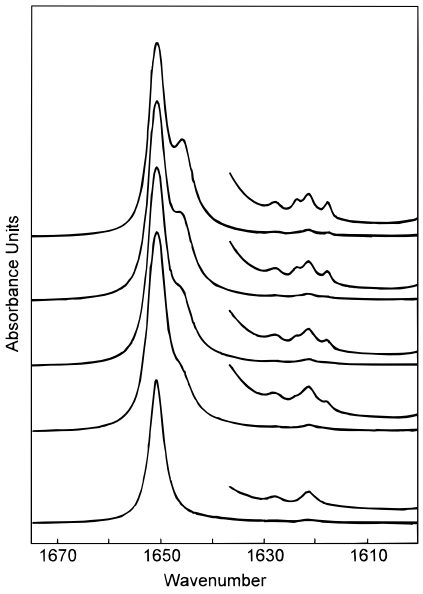

Figure 5. The $\nu_{C=C}$ region of a propene/BF_3 mixture dissolved in liquefied argon. The bottom spectrum was recorded from a solution containing only propene. For the other spectra the temperature of the solution increases from top to bottom : 91.0, 97.9, 101.3 and 104.6 K.

Complex bands were also observed for a number of modes localized in the propene moiety. For example, in Figure 4, the 850−1075 cm^{-1} region of mixed solutions and that of a solution containing only propene are compared. The CH_2 wagging, $\nu_{19}^{C_3H_6}$, at 910 cm^{-1} and the C=C−H out of plane deformation, $\nu_{18}^{C_3H_6}$, at 990 cm^{-1} show blue-shifted complex bands at 925 and 1000 cm^{-1}, respectively. Complex bands, blue shifted by 2−4 cm^{-1}, are also observed for the CH_3 rocking modes $\nu_{17}^{C_3H_6}$ and $\nu_{12}^{C_3H_6}$ at 1043 and 934 cm^{-1}. The weak band at 918 cm^{-1} is assigned to the C−C stretch $\nu_{13}^{C_3H_6}$ in monomer propene. In the spectra of the mixed solutions, a very weak band appears near 921 cm^{-1}, which we assign to the corresponding mode in the complex. Finally, it can be seen in Figure 4 that also for propene/BF_3 mixtures a weak band due to $\nu_1^{BF_3}$ in the complex appears, at 876 cm^{-1}.

The absence of $\nu_2^{C_2H_4}$ in the spectra of monomer ethene makes it difficult to appreciate the complexation shift of the induced complex band. For propene, however, the C=C stretch, $\nu_6^{C_3H_6}$, in the monomer is clearly observed at 1651 cm^{-1}. As can be seen in Figure 5, the corresponding complex mode appears red shifted by 4 cm^{-1}, at 1647 cm^{-1}. Moreover, as can be seen in the same figure, also for the C=C stretch in $CH_3{}^{13}CH{=}CH_2$

Table 4. χ^2 Values for the Stoichiometry Analysis of the Complexes between Ethene and BF_3 and between Propene and BF_3

proposed stoichiometry	ethene/BF_3	propene/BF_3
2:1	0.102	1.575
1:1	0.006	0.026
1:2	0.112	0.232

and $CH_3CH{=}{}^{13}CH_3$, the corresponding complex modes, red shifted over similar distances, have been observed.

Propene/BF_3 mixtures have also been investigated in liquid nitrogen. Also for these solutions, the formation of a propene/BF_3 complex was observed. For the same concentrations of propene and BF_3 as in LAr, the complex bands in LN_2 again are much weaker. This, just as for the ethene complex, suggests also a lower stability of the propene/BF_3 complex in liquid nitrogen than in liquid argon.

2. Stoichiometry of the Observed Species. Using the equilibrium constant for the complexation reaction

$$n\mathrm{RCH{=}CH_2} + m\mathrm{BF_3} \rightleftharpoons (\mathrm{RCH{=}CH_2})_n{\cdot}(\mathrm{BF_3})_m$$

it is easily shown that the integrated intensity $I_{(RCH=CH_2)_n\cdot(BF_3)_m}$ of a band of the complex varies linearly with the product of the monomer intensities $(I_{RCH=CH_2})^n.(I_{BF_3})^m$.[33] This property was used to establish the stoichiometry of the complexes from intensity data obtained from a concentration study. To this end, infrared spectra of several solutions containing concentrations of the appropriate alkene, varying from 5.0×10^{-4} to 2.0×10^{-2} M, and of BF_3, varying from 1.0×10^{-4} to 1.0×10^{-2} M, were recorded at a constant temperature of 98.5 ± 0.3 K.

The integrated intensities required for the analysis were obtained as follows. In both cases, the well-separated $\nu_1^{BF_3} + \nu_3^{BF_3}$ bands in the 2400−2250 cm^{-1} region were used to obtain intensities for monomer BF_3 and for the complex. The integrations were made starting from a least squares band fitting of the region involved. For monomer ethene, the numerically integrated intensity of the $\nu_7^{C_2H_4} + \nu_8^{C_2H_4}$ band was used, while for propene $2\nu_3^{C_3H_6}$ in the same spectral region was used.

The intensities of the complex bands were plotted against the intensity products $(I_{BF_3})^2.(I_{RCH=CH_2})$, $(I_{BF_3}).(I_{RCH=CH_2})$ and $(I_{BF_3}).(I_{RCH=CH_2})^2$. In both cases, a linear graph was only obtained for the plot in which $(I_{BF_3}).(I_{RCH=CH_2})$ was used as abscissa. The χ^2 values for the least-squares straight lines through the experimental points are collected in Table 4. It can be seen that for both complexes the smallest value is observed for the 1:1 intensity product. This shows that the complex band used originates in a 1:1 complex, confirming the anticipated stoichiometry.

3. Complexation Enthalpy of the Observed Species. Using the van't Hoff isochore, and making the usual assumptions,[33] it is easily shown that $\ln[(I_{RCH=CH_2\cdot BF_3})/(I_{RCH=CH_2}){\cdot}(I_{BF_3})]$ must be linearly related to $1/T$, and that the slope of this relation equals $-\Delta H^o/R$, in which ΔH^o is the complexation enthalpy.

To establish ΔH^o, spectra of ethene/BF_3 and propene/BF_3 mixtures in LAr were recorded at several temperatures between 89 and 117 K, and between 88 and 122 K, respectively. Using intensities of monomer and complex species, calculated as described above, van't Hoff plots were constructed. From these plots, shown in Figures 6a and 7a, respectively, and accounting for density variations of the solution,[34] the complexation enthalpies were calculated to be -10.0 ± 0.2 kJ mol^{-1} for ethene·BF_3 and -11.8 ± 0.2 kJ mol^{-1} for propene·BF_3. In agreement with the conclusions obtained from the vibrational spectra, the complexation enthalpy is slightly larger for propene·BF_3.

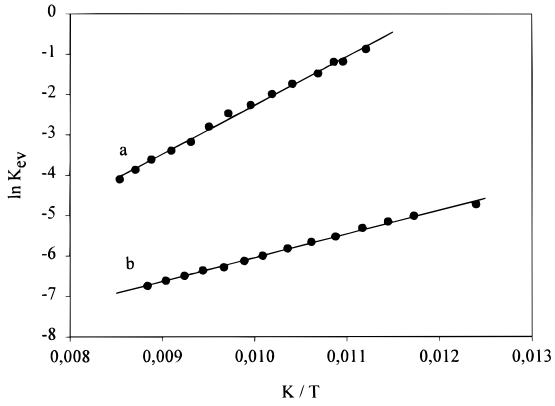

Figure 6. Van't Hoff plots for ethene·BF_3 dissolved in liquefied argon (a) and in liquefied nitrogen (b).

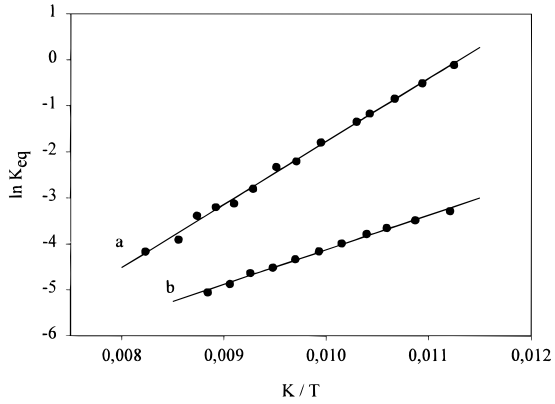

Figure 7. van't Hoff plots for propene·BF_3 dissolved in liquefied argon (a) and in liquefied nitrogen (b).

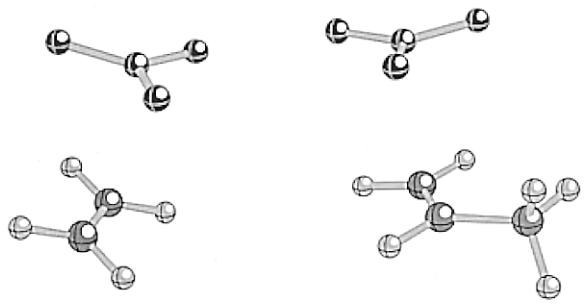

Figure 8. MP2/6-31+G* equilibrium geometries for ethene·BF_3 and propene·BF_3.

Also for solutions in LN_2, temperature studies were carried out. Spectra of ethene/BF_3 and propene/BF_3 mixtures were recorded at several temperatures between 80 and 113 K and between 89 and 113 K, respectively. The presence of the induced N≡N stretch of the solvent, however, prevents an accurate integration of the $\nu_1^{BF_3} + \nu_3^{BF_3}$ band of the complexes. Therefore, the intensity of the $\nu_1^{BF_3}$ and near 880 cm^{-1} was used. The resulting van't Hoff plots are shown Figures 6b and 7b. From these, and accounting for density variations of the solution,[34] the complexation enthalpy was calculated to be -5.4 ± 0.3 kJ mol^{-1} for ethene·BF_3 and -6.9 ± 0.3 kJ mol^{-1} for propene·BF_3. Thus, the complexation enthalpies are much lower than in LAr, the average difference being 4.8 kJ mol^{-1}.

4. *ab Initio* Calculations. Insight into the structure of the complexes was gained from *ab initio* calculations at the MP2/6-31+G* level. In Figure 8, the resulting equilibrium geometries for both ethene·BF_3 and propene·BF_3 are shown. In

(33) Herrebout, W. A.; Van der Veken, B. J. *J. Phys. Chem.* **1994**, *98*, 2836−2843.

(34) Van der Veken, B. J. *J. Phys. Chem.* **1996**, *100*, 17436−17438.

Table 5. MP2/6-31+G* Structural Parameters (Bond Lengths in Å, Bond Angles in Degrees, Dipole Moment in Debye) for ethene·BF_3, for Ethene, and for BF_3[a]

	ethene·BF_3	ethene	BF_3
$r(C_1{=}C_2)$	1.3420	1.3401	
$r(C_2{-}H_3)$	1.0860	1.0857	
$r(C_2{-}H_4)$	1.0858	1.0857	
$r(C_1{-}H_5)$	1.0858	1.0857	
$r(C_1{-}H_6)$	1.0860	1.0857	
$r(C_1{-}X_7)$	0.6710		
$r(X_7{-}B_8)$	2.9221		
$r(B_8{-}F_9)$	1.3303		1.3278
$r(B_8{-}F_{10})$	1.3304		1.3278
$r(B_8{-}F_{11})$	1.3303		1.3278
$\angle(C_1{=}C_2{-}H_3)$	121.497	121.581	
$\angle(C_1{=}C_2{-}H_4)$	121.584	121.581	
$\angle(C_2{=}C_1{-}H_5)$	121.584	121.581	
$\angle(C_2{=}C_1{-}H_6)$	121.497	121.581	
$\angle(C_2{-}X_7{-}C_1)$	180.000		
$\angle(C_2{-}X_7{-}B_8)$	90.000		
$\angle(C_1{-}X_7{-}B_8)$	90.000		
$\angle(B_8{-}X_8{-}C_1)$	90.000		
$\angle(F_9{-}B_8{-}X_7)$	93.680		
$\angle F_{10}{-}B_8{-}X_7)$	87.880		
$\angle(F_{11}{-}B_8{-}X_7)$			
$\tau(H_3{-}C_2{=}C_1{-}H_5)$	179.52	180.00	
$\tau(H_3{-}C_2{=}C_1{-}H_6)$	−0.00	0.00	
$\tau(H_3{-}C_2{=}C_1{-}H_4)$	179.52	180.00	
$\tau(H_4{-}C_2{=}C_1{-}H_5)$	0.00	0.00	
$\tau(H_4{-}C_2{=}C_1{-}H_6)$	−179.52	180.00	
$\tau(H_6{-}C_1{=}C_2{-}H_5)$	179.52	180.00	
$\tau(C_2{-}X_7{-}B_8{-}C_1)$	180.00		
$\tau(B_8{-}X_7{-}C_2{-}H_3)$	−83.95		
$\tau(B_8{-}X_7{-}C_2{-}H_4)$	96.53		
$\tau(B_8{-}X_7{-}C_1{-}H_5)$	−96.53		
$\tau(B_8{-}X_7{-}C_1{-}H_6)$	83.95		
$\tau(F_9{-}B_8{-}X_7{-}C_2)$	150.14		
$\tau(F_{10}{-}B_8{-}X_7{-}C_2)$	90.00		
$\tau(F_{11}{-}B_8{-}X_7{-}C_2)$	−29.86		
dipole moment	0.67	0.00	0.00
energy/Hartree	−402.103990	−78.293243	−323.804151
ΔE_c/kJ mol^{-1}	−17.32		
E_{BSSE}/kJ mol^{-1}	−9.85		
ΔE_c (corr)/kJ mol^{-1}	−7.47		

addition, the structural parameters of the complexes and of the constituent monomers are collected in Tables 5 and 6.

The calculations converge to a structure in which for both complexes the boron atom sits above the π bond of the Lewis base. For ethene, the complex has a symmetry plane perpendicular to the π bond, which contains the boron and one of the fluorine atoms. We will identify the line between the boron atom and the center X of the C=C bond as the van der Waals bond. With respect to the latter, in the ethene complex the BF_3 moiety shows a positive tilt of 3.9°. Similarly, the normal on the plane of the hydrogen atoms of ethene is rotated 6.3 degrees away from the van der Waals bond. Both tilts reflect the sterical hindrance between the fluorine atoms out of the symmetry plane and the opposing hydrogen atoms. This structure is not very rigid, as the barrier to internal rotation around the van der Waals bond is a mere 0.2 kJ mol^{-1}. The complexation energy of the complex is calculated to be −17.32 kJ mol^{-1} without BSSE correction, and −7.47 kJ mol^{-1} with BSSE correction.

Table 5 shows that the complexation has minor influences on the bond lengths of the monomer molecules, which are readily understood from donor−acceptor considerations.[35] The complexation also leads to small deviations from planarity for the constituent molecules in the complex: the B−F bonds make an angle of 1.75° with a plane perpendicular to the symmetry axis of the BF_3 moiety, and the C−H bonds make an angle of 0.2° with the plane through the hydrogen atoms.

(35) Gutman, V. *The Donor Acceptor Approach to Moecular Interactions*; Plenum Press: New York, 1988.

Table 6. MP2/6-31+G* Structural Parameters (Bond Lengths in Å, Bond Angles in Degrees, Dipole Moment in Debye) for Propene·BF_3, for Propene, and for BF_3

	propene·BF_3	propene	BF_3
$r(C_1{=}C_2)$	1.3443	1.3419	
$r(C_2{-}C_3)$	1.4986	1.4994	
$r(C_3{-}H_4)$	1.0938	1.0942	
$r(C_3{-}H_5)$	1.0953	1.0957	
$r(C_3{-}H_6)$	1.0958	1.0957	
$r(C_2{-}H_7)$	1.0904	1.0903	
$r(C_1{-}H_8)$	1.0858	1.0856	
$r(C_1{-}H_9)$	1.0876	1.0874	
$r(C_1{-}X_{10})$	0.5894		
$r(X_{10}{-}B_{11})$	2.8819		
$r(B_{11}{-}F_{12})$	1.3300		1.3278
$r(B_{11}{-}F_{13})$	1.3308		1.3278
$r(B_{11}{-}F_{14})$	1.3320		1.3278
$\angle(C_1{=}C_2{-}C_3)$	124.709	124.590	
$\angle(C_2{-}C_3{-}H_4)$	111.116	110.989	
$\angle(C_2{-}C_3{-}H_5)$	111.077	111.031	
$\angle(C_2{-}C_3{-}H_6)$	110.500	111.031	
$\angle(C_1{=}C_2{-}H_7)$	118.711	118.821	
$\angle(C_2{=}C_1{-}H_8)$	121.528	121.557	
$\angle(C_2{=}C_1{-}H_9)$	121.403	121.486	
$\angle(C_1{-}X_{10}{-}C_2)$	180.000		
$\angle(B_{11}{-}X_{10}{-}C_1)$	90.000		
$\angle(B_{11}{-}X_{10}{-}C_2)$	90.000		
$\angle(F_{12}{-}B_{11}{-}X_{10})$	93.583		
$\angle(F_{13}{-}B_{11}{-}X_{10})$	89.105		
$\angle(F_{14}{-}B_{11}{-}X_{10})$	93.575		
$\angle(F_{12}{-}B_{11}{-}F_{13})$	120.123		120.000
$\angle(F_{12}{-}B_{11}{-}F_{14})$	119.803		120.000
$\angle(F_{13}{-}B_{11}{-}F_{14})$	119.679		120.000
$\tau(C_1{=}C_2{-}C_3{-}H_4)$	3.08	0.00	
$\tau(C_1{=}C_2{-}C_3{-}H_5)$	124.05	−120.49	
$\tau(C_1{=}C_2{-}C_3{-}H_6)$	−117.22	120.49	
$\tau(C_3{-}C_2{=}C_1{-}H_8)$	178.73	180.00	
$\tau(C_3{-}C_2{=}C_1{-}H_9)$	−0.61	180.00	
$\tau(C_3{-}C_2{=}C_1{-}H_7)$	179.00	0.00	
$\tau(H_7{-}C_2{=}C_1{-}H_8)$	−0.28	0.00	
$\tau(H_7{-}C_2{=}C_1{-}H_9)$	−179.61	−180.00	
$\tau(H_9{-}C_1{=}C_2{-}H_8)$	−179.34	−180.00	
$\tau(C_2{-}X_{10}{-}B_{11}{-}C_1)$	180.00		
$\tau(B_{11}{-}X_{10}{-}C_2{-}C_3)$	−89.60		
$\tau(B_{11}{-}X_{10}{-}C_2{-}H_7)$	91.40		
$\tau(B_{11}{-}X_{10}{-}C_1{-}H_9)$	88.99		
$\tau(B_{11}{-}X_{10}{-}C_1{-}H_8)$	−91.67		
$\tau(F_{12}{-}B_{11}{-}X_{10}{-}C_1)$	42.77		
$\tau(F_{13}{-}B_{11}{-}X_{10}{-}C_1)$	−77.36		
$\tau(F_{14}{-}B_{14}{-}X_{10}{-}C_1)$	162.9575		
dipole moment	0.86	0.36	0.00
energy/Hartree	−441.278549	−117.466241	−323.804151
ΔE_c/kJ mol^{-1}	−21.42		
E_{BSSE}/kJ mol^{-1}	−12.05		
ΔE_c (corr)/kJ mol^{-1}	−9.37		

The presence of an extra methyl group in propene leads to an asymmetric complex, for which tilt angles and nonplanarities are more difficult to define, but the data in Table 6 suggest that the effects are slightly more pronounced. This is a consequence of the stronger interaction of propene with BF_3: the complexation energy, with and without BSSE correction, are −21.42 and −9.37 kJ mol^{-1}, respectively.

Discussion

The complexation enthalpies for the BF_3 complexes, −10.0 ± 0.2 kJ mol^{-1} for ethene and −11.8 ± 0.2 kJ mol^{-1} for propene, are slightly higher than those for the HCl complexes which, in LAr, are −8.7 ± 0.2 kJ mol^{-1} [31] and −9.3 ± 0.2 kJ

Table 7. SCRF/SCIPCM Solvatation Energies for Ethene, Propene, BF_3, Ethene·BF_3, and Propene·BF_3[a]

	ΔE_{solv}/kJ mol^{-1}
ethene	0.878
propene	0.808
BF_3	4.134
ethene·BF_3	3.370
propene·BF_3	2.964

[a] All values calculated at the RHF/6-31+G* level.

mol^{-1},[36] respectively. This is not surprising, as BF_3 is known to be a much stronger Lewis acid than HCl. For instance, for CO the ΔH^o for the HCl and the BF_3 complexes are -5.9 ± 0.3 and -8.1 ± 0.3 kJ mol^{-1},[23,37,38] and for CH_3F they are -5.1 ± 0.4 and -16.8 ± 0.5 kJ mol^{-1}.[24,39] These data reveal that the difference in ΔH^o between HCl and BF_3 complexes for ethene and propene is substantially smaller than for the CO and CH_3F complexes. This must be attributed to the higher sterical hindrance in ethene·BF_3 and propene·BF_3.

In agreement with the results obtained for the HCl complexes, for propene·BF_3 the ΔH^o is slightly larger than that for ethene·BF_3. This neatly demonstrates the electron donor character of a methyl group compared to a hydrogen atom.

The complexation enthalpies in LN_2 differ significantly from those in LAr. This is caused by differences in the behavior of BF_3 in both solvents. Monte Carlo simulations[36] suggest that in LN_2 the BF_3 molecules are virtually completely complexed to a 1:2 species N_2·BF_3·N_2, while in LAr the argon atoms merely form a solvation shell. Thus, in LN_2 complexation with ethene or propene requires the breaking of a van der Waals bond between boron and a nitrogen molecule. Neglecting all other effects, the difference in ΔH^o between solutions in LN_2 and LAr then equals the complexation enthalpy for the reaction

$$N_2{\cdot}BF_3 + N_2 \rightleftharpoons N_2{\cdot}BF_3{\cdot}N_2$$

From the results obtained here, this complexation enthalpy can be estimated to be -4.8 ± 0.4 kJ mol^{-1}.

The *ab initio* complexation energies $\Delta E_c^{\text{ab initio}}$ cannot directly be compared with the complexation enthalpies determined in liquid argon. As a first step toward transformation of the ΔH^o into complexation energies, the solvation energies for the monomers and for the complexes in liquid argon were estimated from SCRF/SCIPCM calculations[40] at the RHF/6-31+G* level. These calculations are based on a reaction field model in which the solute/solvent interaction is calculated not only for the solute's dipole moment, but taking into account its full charge distribution, while also the solvent influence on the solute structure is accounted for. These solvation energies, defined as $\Delta E_{solv} = E_{gas} - E_{solution}$, are collected in Table 7. Clearly, the largest solvent stabilization occurs for monomer BF_3. This species has no dipole moment but has important higher multipoles as a consequence of the high bond dipole moments, as will be discussed below. This, combined with the compact form of the molecule, leads to the calculated strong interaction with the solvent.

Strictly spoken, the data in Table 7 are free enthalpies. Assuming solvation entropies are negligible, however, they were equated to solvation enthalpies, and were used to transform the solution complexation enthalpies into vapor phase values ΔH^o_{gas}. This results in a ΔH^o_{gas} of -11.7 ± 0.2 kJ mol^{-1} for ethene·BF_3 and -13.8 ± 0.2 kJ mol^{-1} for propene·BF_3. The uncertainties quoted are those of the solution values. In a next step, the ΔH^o_{gas} were transformed into complexation energies ΔE_c^{exp} values by straightforward statistical thermodynamics, as described before.[31] The corrections were calculated at 100 K, i.e. close to the midpoint of the temperature interval in which the ΔH^o were measured in solution. The resultant ΔE_c^{exp} are -14.2 ± 0.2 kJ mol^{-1} for ethene·BF_3 and -16.3 ± 0.2 kJ mol^{-1} for propene·BF_3. The results show that the thermal contributions to the vapor phase complexation enthalpies tend to destabilize the complexes, and this is enhanced by the solvent influences. The latter obviously is due to the large solvent stabilization of BF_3.

For ethene·BF_3, the uncorrected $\Delta E_c^{\text{ab initio}}$ overestimates ΔE_c^{exp} by 22%, but the BSSE corrected value is only about half the experimental value. A similar pattern, albeit somewhat less pronounced, is found for the propene complex. These results show that there is a reasonable agreement of ΔE_c^{exp} with the uncorrected $\Delta E_c^{\text{ab initio}}$. The much poorer agreement for the BSSE corrected values confirms previous observations[41] that for a truncated basis set the basis set superposition error should be counterbalanced by the basis set incompletness error, which was not done in the present case.

Recently, density functional theory (DFT) has emerged as an alternative to traditional *ab initio* methods.[42−47] Several studies of small hydrogen-bonded and other weakly bound molecular complexes using DFT have been published, and some successes have been claimed.[48−57] Therefore, we have also performed B3LYP/6-31+G* calculations for the ethene complex. The resulting $\Delta E_c^{\text{ab initio}}$ values, with and without BSSE correction, are -8.03 and -6.21 kJ mol^{-1}, respectively. Clearly, the BSSE for the DFT calculations is much smaller. However, even without BSSE corrections the dissociation energy is seriously underestimated. This results underscribes the conclusion by E. Ruiz[58,59] and J. E. Del Bene[60] that for weak molecular complexes further improvements of the functionals used in the DFT calculations are needed.

(36) Herrebout, W. A.: Van der Veken, B. J., unpublished results.
(37) Barri, M. F.; Tokhadze, K. G. *Opt. Spectrossc. (USSR)* **1981**, *51*, 70−73.
(38) Tokhadze, K. G.; and Tkhorzheskaya, N. A. *J. Mol. Struct.* **1992**, *270*, 351−368.
(39) Sluyts, E. J.; Herrebout,W. A.; Van der Veken, B. J. *J. Mol. Struct.* **1994**, *317*, 49−57.
(40) Foresman, J. B.; Keith, T. A.;Wiberg, K. B.; Snoonian, J.; Frish, M. J. *J. Phys. Chem.* **1996**, *100*, 16098−16104.
(41) Jonas, V.; Frenking, G.; Reetz, M. T. *J. Am. Chem. Soc.* **1994**, *116*, 8741−8753.
(42) Parr, R. G.; Yang, W. *Density Functional Theory of Atoms and Molecules*; Oxford University Press: Oxford, 1989.
(43) Dreizler, R. M.; Gross, E. K. U. *Density Functional Theory*; Springer-Verlag: Berlin, 1990.
(44) Labanowski, J. K., Andzelm, J. W., Eds. *Density Functional Methods in Chemistry*; Springer: New York, 1991.
(45) Seminario, J. M.; Politzer, P., Eds. *Modern Density Functional Theory: A Tool for Chemistry*; Elsevier Science, Amsterdam, 1995.
(46) Kohn, W.; Becke, A. D.; Parr, R. G. *J. Phys. Chem.* **1996**, *100*, 12974−12980.
(47) Rauhut, G.; Pulay, P. *J. Phys. Chem.* **1995**, *99*, 3093−3100.
(48) Sim, F.; St-Amant, A.; Papai, I.; Salahub, D. R. *J. Am. Chem. Soc.* **1992**, *14*, 4391−4400.
(49) Latajka, Z.; Bouteiller, Y. *J. Chem. Phys.* **1994**, *101*, 9793−9799.
(50) Kieninge, M.; Suhai, S. *Int. J. Quantum. Chem.* **1994**, *52*, 465−478.
(51) Latajka, Z.; Bouteiller, Y.; Scheiner, S. *Chem. Phys. Lett.* **1995**, *234*, 159−164.
(52) Branchadel, V.; Sbai, A.; Oliva, A. *J. Phys. Chem.* **1995**, *99*, 6472−6476.
(53) Bauschlicher, C. W., Jr.; Ricca, A. *Chem. Phys. Lett.* **1995**, *237*, 14−19.
(54) Jeanvoine, Y.; Bohr, F.; Ruiz-López, M. F. *Can. J. Chem.* **1995**, *73*, 710−715.
(55) Florián, J.; Johnson, B. G. *J. Phys. Chem.* **1995**, *99*, 5899−5908.
(56) Nuvoa, J. J.; Sosa, C. P. *J. Phys. Chem.* **1995**, *99*, 15837−15845.
(57) Chuan Kang, H. *Chem. Phys. Lett.* **1996**, *254*, 135−140.
(58) Ruiz, E.; Salahub, D. R.; Vela, A. *J. Am. Chem. Soc.* **1995**, *117*, 1141−1142.
(59) Ruiz, E.; Salahub, D. R.; Vela, A. *J. Phys. Chem.* **1996**, *100*, 12265−12276.
(60) Del Bene, J. E.; Person, W. B.; Szczepaniak, K. *J. Phys. Chem.* **1995**, *99*, 10705−10707.

Table 8. MP2/6-31+G* Vibrational Frequencies (cm^{-1}) and Infrared Intensities (km mol^{-1}) for Ethene·$^{10}BF_3$, Ethene·$^{11}BF_3$, Ethene, $^{10}BF_3$, and $^{11}BF_3$

description[a]			ethene·$^{11}BF_3$			ethene·$^{10}BF_3$			ethene		$^{11}BF_3$		$^{10}BF_3$	
			$\bar{\nu}$	int	$\Delta\bar{\nu}$	$\bar{\nu}$	int	$\Delta\bar{\nu}$	$\bar{\nu}$	int	$\bar{\nu}$	int	$\bar{\nu}$	int
Ethene Submolecule														
A_g	ν_1	CH_2 sym stretch	3220.0	0.0	−1.1	3220.0	0.0	−1.1	3221.1	−				
	ν_2	C═C stretch	1699.1	0.1	−5.9	1699.1	0.1	−5.9	1705.0	−				
	ν_3	CH_2 scissoring	1405.5	4.4	−1.3	1405.7	0.7	−1.1	1406.8	−				
A_u	ν_4	CH_2 twist	1077.3	0.0	10.4	1077.3	0.0	10.4	1066.9	−				
B_{1g}	ν_5	CH_2 asym stretch	3293.4	0.0	2.6	3293.4	0.0	2.6	3290.8	−				
	ν_6	CH_2 rocking	1264.3	0.0	0.8	1264.3	0.0	0.8	1263.5	−				
B_{1u}	ν_7	CH_2 wagging	1007.7	128.1	25.0	1007.8	126.4	25.0	982.8	133.1				
B_{2g}	ν_8	CH_2 wagging	968.8	0.0	45.5	968.8	0.0	45.5	923.3	−				
B_{2u}	ν_9	CH_2 asym stretch	3317.2	9.2	2.1	3317.2	9.2	2.1	3315.1	20.1				
	ν_{10}	CH_2 rocking	853.1	0.8	0.8	853.1	0.8	0.8	852.3	1.3				
B_{3u}	ν_{11}	CH_2 sym stretch	3205.2	5.4	1.1	3205.2	5.4	1.1	3204.1	12.1				
	ν_{12}	CH_2 scissoring	1513.2	10.1	−1.0	1513.3	13.9	−0.9	1514.2	7.1				
BF_3 submolecule														
A_1'	$\nu_1^{BF_3}$	BF_3 sym stretch	863.4	4.0	−9.0	863.5	4.5	−8.9			872.4	−	872.4	−
A_2''	$\nu_2^{BF_3}$	BF_3 out−of−plane bend	646.4	248.4	−49.2	672.1	269.9	−52.0			695.6	118.0	724.1	127.8
E'	$\nu_3^{BF_3}$	BF_3 asym stretch	1431.2	408.2	−11.4	1483.7	446.4	−11.9			1442.6	483.1	1495.6	524.0
			1429.5	371.9	−13.1	1482.0	399.1	−13.6						
E'	$\nu_4^{BF_3}$	BF_3 in-plane bend	470.3	11.6	−1.7	472.2	11.2	−1.6			472.0	15.2	473.8	14.8
			469.5	9.8	−2.5	471.4	9.5	−2.4						
van der Waals Modes														
			174.9	0.6		174.9	0.6							
			111.2	0.3		111.2	0.3							
			99.6	1.6		99.9	1.5							
			97.2	0.5		97.2	0.5							
			88.0	0.1		88.0	0.1							
			24.2	0.0		24.2	0.0							

[a] Monomer symmetry species and mode numbers are specified.

Although BF_3 and C_2H_4 have zero dipole moments, the value calculated for the complex is 0.67 D. Both structural and induced contributions to this value can be envisaged. The structural contributions primarily originate in the nonplanarity of the BF_3 and the C_2H_4 moieties in the complex. The nonplanarity contributions have been estimated by *ab initio* calculations on the monomers using the geometry they have in the complex. For BF_3, this leads to a dipole moment of 0.21 D, and for C_2H_4 to a value of 0.01 D, both dipole moments nearly parallel to the van der Waals bond. Evidently, the nonplanarity contribution of the ethene moiety can be neglected. The value for BF_3 can be rationalized in terms of bond moments calculated from the charges on the fluorine atoms. A natural bond orbital analysis[61] using the above *ab initio* results leads to charges of −0.518 and −0.515 electrons on the in-plane and out-of-plane fluorine atoms. These charges are in very good agreement with the value of −0.529 electrons reported for monomer BF_3.[62] Using these charges and using the *ab initio* B−F bond lengths, a dipole moment of 0.32 D is then predicted for the BF_3 moiety. This value is not quite the same as the above *ab initio* value, which is a consequence of the approximations used in defining atom charges and bond dipole moments. However, both values are substantially smaller than the dipole moment of the complex, showing that the induced contribution is important as well. From the *ab initio* BF_3 and ethene·BF_3 dipole moments, the induced contribution is calculated to be 0.45 D, and this contribution is also very nearly parallel to the van der Waals bond. No attempts were made to analyze in detail the contributions to this induced moment. However, because of the high charges on the atoms in BF_3, the larger part of the induced dipole moment will reside in the ethene moiety. Altogether, it is clear that the dipole moment of the complex is caused by nonplanarity and induced contributions of similar magnitude. For the propene complex, a similar interpretation emerges.

From the *ab initio* results also the vibrational frequencies and infrared intensities of monomers and complexes have been calculated, and the results, together with the frequency shifts $\Delta\bar{\nu} = \bar{\nu}_{complex} - \bar{\nu}_{monomer}$, are given in Tables 8 and 9.

Comparison of calculated with observed shifts shows that in all cases the *ab initio* calculations predict the correct direction of the shift. However, the agreement is not quantitative. For modes of the BF_3 moiety, with the exception of $\nu_4^{BF_3}$ in the propene complex, the calculated shifts of fundamentals are significantly larger than the observed ones. For instance, the predicted shift for $\nu_2^{^{11}BF_3}$ in ethene·BF_3 is −49.2 cm^{-1}, while the observed shift is −30 cm^{-1}. For combination bands, the shift can be judged by making the approximation it equals the sum of the shifts of the corresponding fundamentals. This approximation is supported by the combination mode $\nu_3^{BF_3} + \nu_4^{BF_3}$ in propene·BF_3: in the ^{11}B isotopomer, the experimental shift for this mode equals −13 cm^{-1}, while the shifts observed for $\nu_3^{BF_3}$ and $\nu_4^{BF_3}$ are −11 and −2 cm^{-1}, respectively. Using this approximation, the *ab initio* shifts of combination bands localized in the BF_3 moiety are found also to be larger, by a similar fraction, than the observed shifts.

For the ethene moiety in ethene·BF_3 a shift is available only for $\nu_7^{C_2H_4} + \nu_8^{C_2H_4}$. Using the same approximation as above, the *ab initio* shift is calculated to be 70.5 cm^{-1}, while the experimental value is 23 cm^{-1}. At least for this ethene mode the calculations overestimate the experimental shift. For propene·BF_3, some of the smaller shifts of propene vibrations are adequately predicted, but the more important shifts, occurring for modes localized near the double bond, experimentally again are much smaller than calculated.

The behavior of the calculated shifts suggests that in the *ab initio* calculations the interaction between BF_3 and ethene is stronger than in the actual complex. As the *ab initio* frequencies

(61) Reed, A. E.; Curtiss, L. A.; Weinhold, F. *Chem. Rev.* **1988**, *88*, 899−926.

(62) Fowler, P. W.; Stone, A. J. *J. Phys. Chem.* **1987**, *91*, 509−511.

Table 9. MP2/6-31+G* Vibrational Frequencies (cm^{-1}) and Infrared Intensities (km mol^{-1}) for Propene·$^{10}BF_3$, Propene·$^{11}BF_3$, Propene, $^{10}BF_3$, and $^{11}BF_3$

description[a]			propene·$^{11}BF_3$			propene·$^{10}BF_3$			propene		$^{11}BF_3$		$^{10}BF_3$	
			$\bar{\nu}$	int	$\Delta\bar{\nu}$	$\bar{\nu}$	int	$\Delta\bar{\nu}$	$\bar{\nu}$	int	$\bar{\nu}$	int	$\bar{\nu}$	int
						$CH_3CH{=}CH_2$ Submolecule								
A′	ν_1	═CH_2 asym stretch	3297.5	7.7	−2.4	3297.5	7.7	−2.4	3295.1	15.4				
	ν_2	═CH stretch	3207.1	8.1	0.8	3207.1	8.1	0.8	3206.3	6.7				
	ν_3	═CH_2 sym stretch	3199.1	13.5	1.7	3199.1	13.6	1.7	3197.4	26.4				
	ν_4	CH_3 asym stretch	3185.3	3.3	6.0	3185.3	3.3	6.0	3179.3	6.0				
	ν_5	CH_3 sym stretch	3090.2	15.3	3.9	3090.2	15.3	3.9	3086.3	21.0				
	ν_6	C═C stretch	1718.0	9.5	−7.5	1718.0	9.8	−7.5	1725.5	9.5				
	ν_7	CH_3 asym deformation	1544.8	15.9	−1.1	1544.9	14.0	−1.0	1545.9	15.9				
	ν_8	═CH_2 deformation	1494.7	1.0	1.2	1495.6	20.3	1.1	1494.5	2.0				
	ν_9	CH_3 sym deformation	1459.8	3.7	0.8	1457.6	40.6	−1.4	1459.0	2.6				
	ν_{10}	C═C−H in-plane deform	1353.3	0.1	1.2	1353.3	0.1	+1.2	1352.1	0.1				
	ν_{11}	═CH_2 rocking	1224.1	0.1	0.9	1224.1	0.1	0.9	1223.2	0.3				
	ν_{12}	CH_3 rocking	973.5	3.2	0.7	973.5	3.2	0.7	972.8	4.0				
	ν_{13}	C−C stretch	956.5	14.9	1.2	956.5	14.7	1.2	955.3	1.5				
	ν_{14}	C═C−C deformation	433.2	0.3	1.1	433.2	0.3	1.1	432.1	0.6				
A″	ν_{15}	CH_2═ asym stretch	3165.6	10.8	5.5	3165.6	10.8	5.5	3160.1	15.0				
	ν_{16}	CH_3 asym deformation	1521.4	10.2	−4.2	1522.0	15.8	−3.6	1525.6	8.6				
	ν_{17}	CH_3 rocking	1099.1	5.4	3.8	1099.1	6.4	3.8	1095.3	4.0				
	ν_{18}	C═C−H out-of-plane	1040.2	21.7	16.5	1040.2	21.4	16.5	1023.7	23.7				
	ν_{19}	═CH_2 wagging	950.4	37.7	35.8	950.5	36.6	35.8	914.7	54.9				
	ν_{20}	═CH_2 twist	609.0	55.4	23.9	609.6	35.8	24.5	585.1	14.6				
	ν_{21}	CH_3 torsion	208.3	1.0	14.6	208.3	1.0	14.6	193.7	0.6				
						BF_3 Submolecule								
A_1'	$\nu_1^{BF_3}$	BF_3 sym stretch	861.5	5.3	−10.9	861.6	6.0	−10.8			872.4	−	872.4	−
A_2''	$\nu_2^{BF_3}$	BF_3 out of plane bend	638.0	224.4	−57.6	662.5	267.0	−61.6			695.6	118.0	724.1	127.8
E′	$\nu_3^{BF_3}$	BF_3 asym. stretch	1431.1	401.9	−11.5	1483.7	387.2	−11.9			1442.6	483.1	1495.6	524.0
			1422.1	351.7	−20.5	1475.3	368.4	−20.3						
E′	$\nu_4^{BF_3}$	BF_3 in plane bend	470.0	11.1	−2.0	471.9	10.8	−1.9			472.0	15.1	473.8	14.8
			469.2	9.3	−2.8	471.0	9.0	2.8						
						van der Waals Modes								
			127.6	0.5		127.7	0.5							
			111.9	0.9		111.9	0.9							
			107.4	2.4		107.6	2.4							
			95.5	0.5		95.6	0.5							
			75.2	0.1		75.3	0.1							
			25.1	0.0		25.1	0.0							

[a] Monomer symmetry species and mode numbers are specified.

were obtained from calculations uncorrected for BSSE, this is in agreement with the above observation that $\Delta E_c^{\text{ab initio}}$ is larger than ΔE_c^{exp}.

The low symmetry of the complexes causes the degeneracy of the antisymmetric BF_3 stretches to be lifted. This, for the ethene complex, leads to a predicted splitting between the two fundamentals of 1.7 cm^{-1}. However, the harmonic *ab initio* calculations do not fully account for the very low barrier toward internal rotation in the complex. Thermal excitation in such a low barrier potential makes that the observed antisymmetric stretches are an average over a complex mixture of initial states, a substantial contribution stemming from molecules excited in torsional levels above the barrier. Instead of giving rise to a well-defined doublet, such an average will collapse into a single, broad band. In agreement with this, in the ethene complex a single band for these modes is observed, the half width of which, at 86.7 K, for the ^{10}B isotope is 2.2 cm^{-1}, while the half width of the corresponding degerate monomer mode is 1.7 cm^{-1}. Due to the stronger interaction, the asymmetry in the propene complex must be more pronounced. The calculated splitting for the antisymmetric stretches in the ^{10}B isotope indeed is 8.4 cm^{-1}, while the experimental half width has increased to 5.1 cm^{-1}.

For both Lewis bases, a relatively small infrared intensity of approximately 5 km mol^{-1} is calculated for the $\nu_1^{BF_3}$ mode in the complex. For propene·BF_3 this intensity is in the same order of magnitude as those for the CH_3 rocking, $\nu_{17}^{C_3H_6}$, and the C═C−H out of plane deformation, ν_{18}, the intensity ratios being 0.32 for the $\nu_1^{BF_3}/\nu_{17}^{C_3H_6}$ and 0.98 for the $\nu_1^{BF_3}/\nu_{18}^{C_3H_6}$ doublet. These ratios compare favorably with the experimental values of 0.24 and 0.90 derived from the vibrational spectra, suggesting that the experimental intensities are correctly accounted for by the calculations.

Finally, it should be noted that also for $\nu_2^{C_2H_4}$ and $\nu_3^{C_2H_4}$ modes in ethene·BF_3, a weak infrared intensity, varying from 0.1 to 4.4 km mol^{-1} was predicted. For $\nu_2^{C_2H_4}$, such a band was indeed observed. However, in none of the spectra, a band due to the $\nu_3^{C_2H_4}$ mode in ethene·BF_3 was observed, presumably because it is strongly overlapped by the $\nu_1^{BF_3} + \nu_4^{BF_3}$ band of monomer BF_3.

Acknowledgment. W.A.H. is indebted to the Fund for Scientific Research (FWO, Belgium) for an appointment as Postdoctoral Fellow. The FWO is also thanked for financial help toward the spectroscopic equipment used in this study. Financial support by the Flemish Community, through the Special Research Fund (BOF), is gratefully acknowledged.

JA971887A